Central Retinal Vascular Trunk Deviation in Unilateral Open-angle Glaucoma

Kyoung Min Lee
Boramae Medical Center
Martha Kim
Dongguk University Ilsan Hospital
Sohee Oh
Boramae Medical Center
Seok Hwan Kim (xcski@hanmail.net)
Boramae Medical Center

Research Article

Keywords: open-angle glaucoma (OAG), eye, locoregional susceptibility factor, eyeball expansion

Posted Date: December 23rd, 2020

DOI: https://doi.org/10.21203/rs.3.rs-123828/v1

Abstract

Patients with unilateral open-angle glaucoma (OAG) have suffered glaucomatous optic neuropathy in one eye only despite shared systemic factors between two eyes. It suggests a locoregional susceptibility factor associated with glaucoma development. In this study, we measured the distance of the central retinal vascular trunk from the Bruch's membrane opening (BMO) center relative to that of the BMO margin: the shift index, since it can be used as a surrogate of lamina cribrosa (LC) shift caused by different growth between retinal and scleral layers during eyeball expansion. The shift index was compared between OAG and fellow control eyes within individuals (129 OAG patients). Although OAG eyes also had higher baseline IOP, a larger β-zone parapapillary atrophy area, a larger shift index was the only risk factor of OAG diagnosis in a generalized linear mixed-effects model. Further, a generalized estimating equation regression model revealed that the shift index was larger in the OAG eyes than in the control eyes for all ranges of axial length, while it was the smallest for the axial length of 23.7 mm. Thus, a larger shift index and LC shift may act as a locoregional susceptibility factor for unilateral OAG eyes.

Introduction

Glaucoma is characterized by progressive axonal loss of retinal ganglion cells[1–3]. Many factors such as mechanical, ischemic, metabolic, and immunologic insults have been nominated as candidate sources of axonal damage[1–3]. So far, intraocular pressure (IOP) is the only controllable factor, but it cannot explain every aspect of glaucoma. To be specific, in many cases, glaucomatous damage starts with a localized retinal nerve fiber layer (RNFL) defect, whereas IOP affects the optic nerve head (ONH) universally. This suggests a loco-regional susceptibility factor that makes some parts of the ONH more vulnerable to damage.

The lamina cribrosa (LC) is the principal site of axonal injury in glaucoma[4]. Therefore, LC change might be involved in increased loco-regional susceptibility. In the recent Boramae Myopia Cohort Study, we found that axial elongation evoked LC shift, in contrast to the relative preservation of the Bruch's membrane opening (BMO)[5–7]. In subsequent studies with myopic open-angle glaucoma (OAG), the direction of LC shift from the BMO center showed a strong spatial correlation with the initial hemispheric location of glaucomatous damage[8,9]. This indicated that LC shift might reflect the loco-regional susceptibility of the ONH.

Besides the initial asymmetric hemispheric involvement of glaucomatous damage, unilateral involvement of glaucoma is often encountered. Even if fellow eyes are not normal and might, therefore, be affected by glaucoma in the future, unilateral glaucoma eyes are the best subjects to be scrutinized for loco-regional susceptibility factors after adjusting for systemic factors within a subject at the time of study. The purpose of the present study was to determine whether the position of the central retinal vascular trunk, as a surrogate of LC shift, increases susceptibility to glaucomatous damage in unilateral OAG patients while other systemic risk factors are controlled by inter-eye comparison within the same subject.

Results

This study initially involved 154 unilateral OAG patients. Of these, 9 patients were excluded due to poor image quality of radial scans leading to incomplete visualization of the BMO margin, and 6 patients were excluded owing to bifurcation of central retinal vascular trunk on emergence. The emergence of the vascular trunk was not visible in 24 patients on infrared imaging. Among these, 14 patients were proved to not have the vascular trunk within the BMO by fluorescein or OCT angiography and they were included, while 6 who had not undergone angiography were excluded. Four patients who had the vascular trunk outside the BMO in both eyes were also excluded, leaving a final sample of 129 unilateral OAG patients. The subjects were aged 55.6 ± 14.6 years, 62 of whom were female (48%).

As compared with the respective fellow control eyes, OAG eyes had higher baseline IOP (14.9 ± 3.7 mmHg vs. 14.2 ± 2.8 mmHg, $P < 0.001$), longer axial length (25.1 ± 1.6 mm vs. 24.9 ± 1.5 mm, $P < 0.001$), and worse visual field parameters (mean deviation: -4.21 ± 3.53 dB vs. -1.04 ± 1.60 dB, $P < 0.001$; pattern standard deviation: 5.47 ± 3.95 dB vs. 1.99 ± 0.85 dB, $P < 0.001$) (Table 1). Both the area of the BMO (2.68 ± 0.71 mm^2 vs. 2.60 ± 0.67 mm^2, $P = 0.014$) and that of β-zone PPA (1.01 ± 0.70 mm^2 vs. 0.88 ± 0.67 mm^2, $P = 0.001$) were larger in the OAG eyes than in the fellow control eyes. The shift index also was larger in the OAG eyes (0.55 ± 0.28 vs. 0.37 ± 0.22, $P < 0.001$), while the angular deviation of vascular trunk did not differ between the groups (15.4 ± 69.4° vs. 3.9 ± 68.1°, $P = 0.147$). The GLMM analysis revealed that larger shift index was the only risk factor for OAG diagnosis (OR = 8.705, $P = 0.001$) (Table 2).

Table 1
Demographic comparison between glaucoma and fellow control eyes

	Glaucoma eye (N = 129)	**Fellow control eye (N = 129)**	***P****
Baseline IOP, *mmHg*	14.9 ± 3.7	14.2 ± 2.8	< 0.001
Axial length, *mm*	25.1 ± 1.6	24.9 ± 1.5	< 0.001
Angular deviation of vascular trunk, *°*	15.4 ± 69.4	3.9 ± 68.1	0.147
Shift index	0.55 ± 0.28	0.37 ± 0.22	< 0.001
BMO area, mm^2	2.68 ± 0.71	2.60 ± 0.67	0.014
β-zone PPA area, mm^2	1.01 ± 0.70	0.88 ± 0.67	0.001
Mean deviation, *dB*	-4.21 ± 3.53	-1.04 ± 1.60	< 0.001
Pattern standard deviation, *dB*	5.47 ± 3.95	1.99 ± 0.85	< 0.001
IOP = intraocular pressure; BMO = Bruch's membrane opening; PPA = parapapillary atrophy			
*Comparison performed using paired *t*-test.			

Table 2
Factors associated with presence of glaucoma within each subject.

	Univariable analysis			**Multivariable analysis***		
	OR	95% CI	*P*	OR	95% CI	*P*
Baseline IOP, *mmHg*	1.062	(0.983, 1.147)	0.127	1.072	(0.983, 1.167)	0.115
Axial length, *mm*	1.063	(0.908, 1.245)	0.445			
Angular deviation of vascular trunk, °	1.003	(0.999, 1.007)	0.172	1.003	(0.999, 1.007)	0.121
Shift index	**15.927**	**(5.510, 46.040)**	**< 0.001**	**8.705**	**(2.554, 29.675)**	**0.001**
BMO area, mm^2	1.178	(0.824, 1.684)	0.370			
β-zone PPA area, mm^2	1.344	(0.930, 1.941)	0.115	0.967	(0.643, 1.453)	0.870

OR = odds ratio; CI = confidence interval; IOP = intraocular pressure; BMO = Bruch's membrane opening; PPA = parapapillary atrophy

Statistically significant values ($P < 0.05$) are shown in bold. *Variables with $P < 0.20$ in the univariate analysis were included in the subsequent multivariate analysis. Paired eye correlation was adjusted using the generalized linear mixed-effects model.

The shift index varied according to the diagnosis and axial length (Fig. 1A). The OAG group had a larger shift index than the fellow control group for all ranges of axial length. Regarding the effect of axial length, the shift index showed a non-linear relationship with the lowest value at the axial length of 23.7 mm. From this point, the shift index increased in either direction of axial length change (Fig. 1A, red dashed vertical line). To evaluate the effect of both factors while accounting for the paired-eye correlations, the GEE regression model was fitted to the data set (Table 3). The equation was constructed as first-, second-, and third-order terms of the axial length and first-order term of the diagnosis. It corresponded to J-shaped curves according to axial length and showed an independent effect of diagnosis on the shift index (Table 3).

The OAG eyes had a larger shift index than did the fellow eyes in cases either of nasally located vascular trunk (Fig. 2A–C) or temporally located vascular trunk (Fig. 3A–C). To compare the intra-individual difference of shift index and β-zone PPA area, those parameters of the fellow control eyes were subtracted from those of the OAG eyes (Fig. 1B). In contrast to the β-zone PPA area, the shift index was consistently larger in the OAG eyes than in the fellow control eyes over the entire range of axial length (Fig. 1B).

The angular deviation of the vascular trunk showed a correlation with the angular location of RNFL defect in the total group (r=-0.423, P< 0.001) and in the subgroup with the temporal location of vascular trunk (r=-0.539, P = 0.010).

Discussion

Newborns have their vascular trunk in the central area of the ONH in most cases[10]. In the Boramae Myopia Cohort Study, we demonstrated actual shifting of vascular trunk in contrast to the preserved BMO during myopic axial elongation[5–7]. Because the central retinal vascular trunk is embedded in the dense connective tissue of the LC[11], shift and deviation of the vascular trunk from the BMO center would be related to shift of the underlying LC. Moreover, vascular trunk deviation from the BMO center is closely related to the location of optic nerve damage in myopic OAG patients[8,9]. This could be an explanation for the close association between vascular trunk location and the location of glaucomatous damage, which were reported in many other reports[12–15]. Taken together, LC shift on the en-face plane, possibly as the reason of vascular trunk deviation from the BMO center, could reflect stress exerted on the LC. In the present study, we found that the vascular trunk position was deviated farther from the BMO center in glaucoma eyes than in fellow control eyes in unilateral OAG patients. This implies that a more shifted LC might be more susceptible to glaucomatous damage than a less shifted LC within the same subject.

To evaluate the effect of LC shift on glaucoma development, we included exclusively unilateral OAG patients having one glaucoma eye and one non-glaucoma eye. In this manner, we could exclude the effects of systemic factors such as aging and other general health-related conditions[16]. Subsequently, we focused on the local factors that make eyes more susceptible to glaucomatous damage. Although, the fellow eyes of unilateral OAG patients might differ from the healthy eyes, and unilaterality might exist only within a limited period of time[17], our study, at the time of its conduct, informed us which eye was more susceptible to damage: the eye with larger LC shift was affected by glaucomatous damage earlier than the fellow eye with smaller LC shift. This might explain why glaucoma occurs in the eye that it does, only under the same systemic risk factors and similar IOP.

Shift of the LC can increase the susceptibility of the ONH to glaucomatous damage, because it reflects the tangential stress that had been applied to the ONH during eyeball growth[5–9]. Interestingly, in the present study, LC shift did not show a linear correlation with axial length (Fig. 1A). Rather, the correlation between LC shift and axial length was a J-shaped curve, and the GEE regression model showed that the shift index was the smallest for the axial length of 23.7 mm (Table 3), from which point, it increases in either direction. This could be understood by the various shapes of ocular expansion during growth[18]. The average axial length of newborns is around 17 mm, which is about 7 mm shorter than that of adults[19]. This means that every eyeball has to grow after birth, regardless of how short it will be in adulthood. Therefore, the process of outer-wall shift would not be limited to myopic eyes only, but would manifest in eyes of larger-than-17 mm axial length as well. In contrast to the prolate (= axial overgrowth) growth of myopic eyes[18,20], some eyes, especially hyperopic ones, have been reported to have oblate

growth[18,21]. We speculated that oblate growth in hyperopic eyes would lead to the temporal shift of the outer-wall, which could be the cause of shift index increase in the reverse direction in eyes of axial length less than 23.7 mm (Fig. 1A).

Our study showed that such a shift, across the entire range of axial length, was larger in the OAG group than in the control group (Table 3). The GEE regression model revealed that the shift index of the OAG eye was larger than that of the control eye for a given axial length (Fig. 1A). This suggested that the OAG eyes had to endure more shifting than the control eyes with similar axial lengths. Therefore, LC shift could be an indicator of cumulative tensile stress exerted on the LC during growth, and not in myopic eyes only but in any eyes.

It should be noted that the direction of LC shift was associated with the location of glaucomatous damage in cases either of nasal or temporal shift. The large pores of the LC in the superior and inferior regions are considered to be more susceptible to glaucomatous damage[4,11,22]. Moreover, the LC is reported to have a horizontal ridge[11,23], which might protect the LC from tensile stress acting parallel to it. Therefore, we speculated that tensile stress would converge to the susceptible pores in the superior and inferior regions [8,9], even if the direction of LC shift was nearly parallel to the horizontal meridian.

Park et al. showed by means of a subgroup analysis that β-zone-PPA-associated variables could be risk factors for unilateral normal-tension glaucoma[24]. Also in our study, the β-zone PPA area was larger in the OAG group, though it was not significant in the multivariable analysis. In our previous study, we showed that a part of β-zone PPA, which is to say, not only γ-zone PPA but also some of β-zone PPA with Bruch's membrane, appeared as the manifestation of LC and scleral shifting beneath the preserved BMO[7]. In this type of β-zone PPA, the extent of LC shift, as measured by vascular trunk dragging, was larger than the extent of β-zone PPA change[7]. Therefore, in this study, the effect of β-zone PPA might have been smeared out by the larger amount of vascular trunk deviation, which is more representative of LC shift (Fig. 1B)[7]. The following implication of β-zone PPA, however, should be noted: at least in some eyes, larger β-zone PPA would represent a larger LC shift below the BMO, which makes the ONH more susceptible to a second insult such as increased IOP or other tissue-toxic factors[1,3].

In the present study's multivariable analysis, baseline IOP was not the factor associated with OAG presence. This can be explained in two ways. First, most of the OAG patients in this study had baseline IOP within the normal range: normal-tension glaucoma. Second, even in the presence of unilateral OAG, the baseline IOPs of the subjects were highly correlated with each other ($r = 0.883$, $P < 0.001$). Therefore, the intra-individual difference of IOP was too small to make any substantial effect. This, however, should not be interpreted to mean that IOP is not an important factor. LC shift might make the ONH more susceptible to fundamental IOP-mediated insult. Furthermore, the concept of LC shift could explain why IOP reduction is the most effective treatment for OAG, even in cases of normal IOP. IOP lowering can reduce not only the direct IOP-related axial force but also the tensile stress exerted on the outer load-bearing structures, which could act as a tangential force exacerbating, by the shearing effect, damage to

the ONH. Since growth-acquired shift cannot be reversed, additional stress in susceptible eyes with large LC deviation should be reduced instead, especially in cases of evident glaucoma progression.

This study has several limitations. First, the study design was cross-sectional. As such, we could not demonstrate actual LC shifting during earlier growth periods. The premise of this study was based on our previous prospective cohort study results[5–7]. Thus, we cannot exclude the possibility of confounding effect of LC remodeling on the CRVT position in the OAG eyes. However, glaucomatous ONH change has been reported not to affect the position of the CRVT in the LC portion[9,25]. Second, the location of the vascular trunk within the BMO, which was used as the indicator of LC shift, has a limitation. Since the vascular trunk outside the BMO could not be visualized with angiography, the extent of LC shift could be underestimated in such cases. Moreover, some eyes showed bifurcation of the vascular trunk on its emergence. Since we excluded such cases, we did not have any means of measuring the LC shift in those eyes. Additionally, the initial location of the vascular trunk was presumed to be the BMO center, which would not be certain for all eyes. However, most newborns had the central retinal vascular trunk in the center of the optic disc[10], and the hyaloid artery is reported to be in the middle of the orbital part of the nerve when the back of the globe is formed in the embryo state[26]. Finally, we exclusively included subjects with unilateral OAG. Unilateral and bilateral OAG patients might have different characteristics[16]. Patients with systemic risk factors might have bilateral glaucomatous damage[16], though they were selectively excluded from this study. Therefore, our relevant study results should be interpreted with caution.

In conclusion, the LC had been shifted farther from the BMO center in the glaucoma eye than in the fellow control eye of unilateral OAG patients. Larger LC shift might represent the larger cumulative stress exerted on the ONH during growth, which makes the ONH more susceptible to additional insults induced by increased IOP or other factors.

Methods

This investigation was based on OAG patients included in the Boramae Glaucoma Imaging Study (BGIS), an ongoing prospective study at Seoul National University Boramae Medical Center (Seoul, Korea). Written informed consent to participate was obtained from all of the subjects. The study protocol was approved by the Seoul National University Boramae Medical Center Institutional Review Board and conformed to the tenets of the Declaration of Helsinki.

All of the participants underwent a full ophthalmologic examination that included best-corrected visual acuity (BCVA) assessment, refraction, slit-lamp biomicroscopy, Goldmann applanation tonometry, gonioscopy, dilated funduscopic examination, keratometry (RKT-7700; Nidek, Hiroshi, Japan), axial length measurement (IOLMaster version 5; Carl Zeiss Meditec, Dublin, CA, USA), disc photography and red-free fundus photography (TRC-NW8; Topcon, Tokyo, Japan), spectral-domain (SD) OCT (Spectralis OCT, Heidelberg Engineering, Heidelberg, Germany) and standard automated perimetry (Humphrey Field Analyzer II 750, 24-2 Swedish Interactive Threshold Algorithm; Carl-Zeiss Meditec, Dublin, CA, USA).

During the acquisition of SD-OCT images, the subjects were asked to fixate on the target, and images were acquired with the forehead and chin stabilized by the headrest. Extra care was taken during each exam to confirm that the forehead and chin were correctly positioned and did not move. Prior to treatment, IOP was measured repeatedly (typically five times) on the same or different days. The average value, which was defined as the baseline IOP, was used for the subsequent analysis.

Glaucomatous optic nerve damage was defined as rim thinning, notching and the presence of RNFL defects, and was evaluated by a glaucoma specialist (SHK). OAG was defined as glaucomatous optic nerve damage and associated visual field defects, and an open iridocorneal angle (in the case of cataract surgery, the angle was confirmed preoperatively). Glaucomatous visual field defect was defined as (1) outside normal limits on glaucoma hemifield test, or (2) three abnormal points, with a *p* value less than 5% probability of being normal and one with a *p* value less than 1% by pattern deviation, or (3) pattern standard deviation of less than 5%. Visual field defects were confirmed on two consecutive reliable tests (fixation loss rate of $\leq$ 20%, and false-positive and false-negative error rates of $\leq$ 25%).

The inclusion criteria were unilateral OAG patients. To be specific, the contralateral eye for each patient had to have a normal optic disc appearance, an open iridocorneal angle, a normal red-free fundus photograph, and a normal visual field. The exclusion criteria were BCVA of < 20/40, a sharply defined posterior staphyloma (which can deform the contour of the eyeball) on funduscopic examination, a history of ocular surgery other than cataract extraction or corneal refractive surgery, retinal or neurologic disease other than glaucoma that could cause visual field defect, a poor-quality image (i.e., quality score <15) of any section on enhanced depth imaging (EDI) SD-OCT radial scans, and a central retinal vascular trunk position located within the BMO but impossible to determine clearly due to vessel bifurcation. OAG eyes were compared with their fellow control eyes.

Assessment of the central retinal vascular trunk position

Our strategy for demarcation of BMO and vascular trunk position has been described previously[8,9]. The peripapillary area was imaged by SD-OCT (Spectralis, Heidelberg Engineering) using the EDI technique. Possibility of the magnification error was prevented by entering the corneal curvature of each eye into the SD-OCT system before scanning. The BMO was demarcated using the Glaucoma Module Premium Edition of the Spectralis machine. With 24 high-resolution radial scan images of the ONH, 15° apart from each other, each averaged from 24 individual B-scans, SD-OCT automatically detects the margin of the BMO. Every detected BMO margin was reviewed by one of the authors (KML), and errors were corrected manually. Based on the edited BMO margin, the Spectralis machine calculated the area and center of the BMO.

The vascular trunk position was determined in the same way of our previous studies[8,9]. First, the location of the vascular trunk was demarcated on fundoscopic infrared images and color-disc photography (Fig. 4A&B). Then, its location was confirmed by cross-sectional SD-OCT imaging in all cases. If a vascular

trunk was not visible on either infrared fundus photographs or B-scan EDI SD-OCT images, fluorescein or OCT angiography (Spectralis) was used to determine the presence of the vascular trunk within the BMO. The position of the vascular trunk was defined in two aspects: 1) its angular deviation (Fig. 4B, α), and 2) the extent of shift (Fig. 4B, *a*). The angle was measured based on the right-eye orientation, with the nasal horizontal midline as 0° (a positive value indicating a vascular trunk located superiorly, and a negative value indicating a vascular trunk located inferiorly). To evaluate the extent of shift, the distance of the vascular trunk from the center of the BMO (*a*) was divided by the distance of the BMO margin from the center of the BMO in that direction (*b*), and defined as 'shift index' (Fig. 4B, *a*/*b*). In cases of invisible vascular trunk due to being located outside the BMO, the shift index was defined as 1.0, and the angular deviations were not determined. Using the Image J program (version 1.51, National Institutes of Health, Bethesda, MD, USA), one of the authors (KML), who as blinded to the participants' clinical information, measured the distances and angles. The reproducibility of the locating of the central retinal vascular trunk was excellent, as we had stated in the previous study[8].

Assessment of RNFL defects

The angular location of RNFL defect was defined in the same image used for the vascular trunk localization based on the right-eye orientation[8]. First, an infrared fundus image was overlapped with a red-free fundus photograph using commercial software (Photoshop; Adobe, San Jose, CA, USA) (Fig. 4C). The points where the boundaries of the RNFL defect meet the BMO margin were determined. The angular location of the midpoint of the RNFL defect on the BMO margin was measured from the center of the BMO, with the temporal horizontal midline as 0° (a positive value indicating an RNFL defect located superiorly, and a negative value indicating an RNFL defect located inferiorly) (Fig. 4B, β). In cases of RNFL defect in both hemispheres, the angular location was measured to the larger RNFL defect based on the angular width.

Assessment of parapapillary atrophy

β-zone parapapillary atrophy (PPA) was defined as the area without any retinal pigment epithelium (RPE) adjacent to the ONH. The β-zone PPA area was measured on the same infrared OCT fundus images by one observer (KML) blinded to the subjects' information. Using the built-in caliper tool of the Spectralis OCT system, two boundaries were drawn: 1) the RPE opening (RPEO), which is the area without the RPE, and 2) the clinical disc margin (CDM). The β-zone PPA area was defined as the RPEO area minus the CDM area[7].

Data analysis

The paired *t*-test was used for the intraindividual comparison between the OAG and fellow control eyes. Subgroup analyses were performed by the Mann-Whitney U test and Wilcoxon signed-rank test. To

account for the paired-eye correlation, a generalized linear mixed-effects model (GLMM) was used for univariable and multivariable analyses. Parameters with a *P* value less than 0.20 in the univariable analysis were included in the subsequent multivariable analysis. A locally weighted scatterplot smoothing (LOESS) curve was fitted to the data. The LOESS curve uses iterative weighted least squares to determine values that best fit the data[27]. A generalized estimating equation (GEE) regression model was applied to simulate the shift index change according to the glaucoma diagnosis and axial length while controlling for paired-eye correlations. Statistical analyses were performed with commercially available software (Stata version 14.0; StataCorp, College Station, TX, USA) and R statistical packages version 3.4.3 (available at http://www.r-project.org; assessed December 5, 2017). The data herein are presented as the mean ± standard deviation except where stated otherwise, and the cutoff for statistical significance was set at $P < 0.05$.

Declarations

Acknowledgment

a. Funding/Support:

This work was supported by the KIST Institutional Program (2E30140). The funders had no role in study design, data collection and analysis, decision to publish, or preparation of the manuscript.

b. Financial Disclosures:

Kyoung Min Lee: None; Martha Kim: None; Sohee Oh: None; Seok Hwan Kim: None.

c. Other Acknowledgements:

None.

Synopsis

Unilateral open-angle glaucoma patients had a more deviated vascular trunk in the glaucoma eye than in the fellow control eye. Lamina cribrosa shift, as inferred from vascular trunk shift, would increase susceptibility to glaucoma.

References

1. Weinreb, R. N., Aung, T. & Medeiros, F. A. The pathophysiology and treatment of glaucoma: a review. *JAMA* **311**, 1901–1911, doi:10.1001/jama.2014.3192 (2014).

2. Burgoyne, C. F. A biomechanical paradigm for axonal insult within the optic nerve head in aging and glaucoma. *Exp Eye Res* **93**, 120–132, doi:10.1016/j.exer.2010.09.005 (2011).
3. Quigley, H. A. Glaucoma. *Lancet* **377**, 1367–1377, doi:10.1016/s0140-6736(10)61423-7 (2011).
4. Quigley, H. A., Addicks, E. M., Green, W. R. & Maumenee, A. E. Optic nerve damage in human glaucoma. II. The site of injury and susceptibility to damage. *Arch Ophthalmol* **99**, 635–649 (1981).
5. Kim, M., Choung, H. K., Lee, K. M., Oh, S. & Kim, S. H. Longitudinal Changes of Optic Nerve Head and Peripapillary Structure during Childhood Myopia Progression on OCT: Boramae Myopia Cohort Study Report 1. *Ophthalmology* **125**, 1215–1223, doi:10.1016/j.ophtha.2018.01.026 (2018).
6. Lee, K. M., Choung, H. K., Kim, M., Oh, S. & Kim, S. H. Positional Change of Optic Nerve Head Vasculature during Axial Elongation as Evidence of Lamina Cribrosa Shifting: Boramae Myopia Cohort Study Report 2. *Ophthalmology* **125**, 1224–1233, doi:10.1016/j.ophtha.2018.02.002 (2018).
7. Lee, K. M., Choung, H. K., Kim, M., Oh, S. & Kim, S. H. Change of beta-Zone Parapapillary Atrophy During Axial Elongation: Boramae Myopia Cohort Study Report 3. *Invest Ophthalmol Vis Sci* **59**, 4020–4030, doi:10.1167/iovs.18-24775 (2018).
8. Lee, K. M., Kim, M., Oh, S. & Kim, S. H. Position of Central Retinal Vascular Trunk and Preferential Location of Glaucomatous Damage in Myopic Normal-Tension Glaucoma. *Ophthalmology Glaucoma* **1**, 32–43, doi:https://doi.org/10.1016/j.ogla.2018.05.003 (2018).
9. Lee, K. M., Kim, M., Oh, S. & Kim, S. H. Hemisphere opposite to vascular trunk deviation is earlier affected by glaucomatous damage in myopic high-tension glaucoma. *PLoS One* **15**, e0233270, doi:10.1371/journal.pone.0233270 (2020).
10. Kim, M., Kim, S. Y., Lee, K. M., Oh, S. & Kim, S. H. Position of Central Vascular Trunk and Shape of Optic Nerve Head in Newborns. *Invest Ophthalmol Vis Sci* **60**, 3381–3387, doi:10.1167/iovs.19-27363 (2019).
11. Quigley, H. A. & Addicks, E. M. Regional differences in the structure of the lamina cribrosa and their relation to glaucomatous optic nerve damage. *Arch Ophthalmol* **99**, 137–143 (1981).
12. Jonas, J. B. *et al.* Central retinal vessel trunk exit and location of glaucomatous parapapillary atrophy in glaucoma. *Ophthalmology* **108**, 1059–1064, doi:10.1016/s0161-6420(01)00571-1 (2001).
13. Huang, H. *et al.* Position of the central retinal vessel trunk and pattern of remaining visual field in advanced glaucoma. *Br J Ophthalmol* **97**, 96–100, doi:10.1136/bjophthalmol-2012-302068 (2013).
14. Wang, M. *et al.* Relationship Between Central Retinal Vessel Trunk Location and Visual Field Loss in Glaucoma. *Am J Ophthalmol* **176**, 53–60, doi:10.1016/j.ajo.2017.01.001 (2017).
15. Shon, K. *et al.* Nasalization of Central Retinal Vessel Trunk Predicts Rapid Progression of Central Visual Field in Open-Angle Glaucoma. *Sci Rep* **10**, 3789, doi:10.1038/s41598-020-60355-1 (2020).
16. Kim, C. & Kim, T. W. Comparison of risk factors for bilateral and unilateral eye involvement in normal-tension glaucoma. *Invest Ophthalmol Vis Sci* **50**, 1215–1220, doi:10.1167/iovs.08-1886 (2009).
17. Kim, D. W. *et al.* Prelamina and Lamina Cribrosa in Glaucoma Patients With Unilateral Visual Field Loss. *Invest Ophthalmol Vis Sci* **57**, 1662–1670, doi:10.1167/iovs.15-18453 (2016).

18. Lee, K. M., Park, S.-W., Kim, M., Oh, S. & Kim, S. H. Relationship between 3D-MRI Eyeball shape and Optic Nerve Head Morphology. *Ophthalmology*, doi:10.1016/j.ophtha.2020.08.034 (2020).
19. Gordon, R. A. & Donzis, P. B. Refractive development of the human eye. *Arch Ophthalmol* **103**, 785–789, doi:10.1001/archopht.1985.01050060045020 (1985).
20. Atchison, D. A. *et al.* Shape of the retinal surface in emmetropia and myopia. *Invest Ophthalmol Vis Sci* **46**, 2698–2707, doi:10.1167/iovs.04-1506 (2005).
21. Mutti, D. O., Sholtz, R. I., Friedman, N. E. & Zadnik, K. Peripheral refraction and ocular shape in children. *Invest Ophthalmol Vis Sci* **41**, 1022–1030 (2000).
22. Quigley, H. A., Hohman, R. M., Addicks, E. M., Massof, R. W. & Green, W. R. Morphologic changes in the lamina cribrosa correlated with neural loss in open-angle glaucoma. *Am J Ophthalmol* **95**, 673–691 (1983).
23. Park, S. C. *et al.* Horizontal central ridge of the lamina cribrosa and regional differences in laminar insertion in healthy subjects. *Invest Ophthalmol Vis Sci* **53**, 1610–1616, doi:10.1167/iovs.11-7577 (2012).
24. Park, S. C., Lee, D. H., Lee, H. J. & Kee, C. Risk factors for normal-tension glaucoma among subgroups of patients. *Arch Ophthalmol* **127**, 1275–1283, doi:10.1001/archophthalmol.2009.247 (2009).
25. Wang, B. *et al.* Location of the Central Retinal Vessel Trunk in the Laminar and Prelaminar Tissue of Healthy and Glaucomatous Eyes. *Sci Rep* **7**, 9930, doi:10.1038/s41598-017-10042-5 (2017).
26. Haden, H. C. The Development of the Ectodermal Framework of the Optic Nerve, With Especial Reference to the Glial Lamina Cribrosa. *Transactions of the American Ophthalmological Society* **44**, 61–64 (1946).
27. Cleveland, W. S. & Devlin, S. J. Locally Weighted Regression: An Approach to Regression Analysis by Local Fitting. *Journal of the American Statistical Association* **83**, 596–610, doi:10.1080/01621459.1988.10478639 (1988).

Table

Due to technical limitations, table 3 is only available as a download in the Supplemental Files section.

Figures

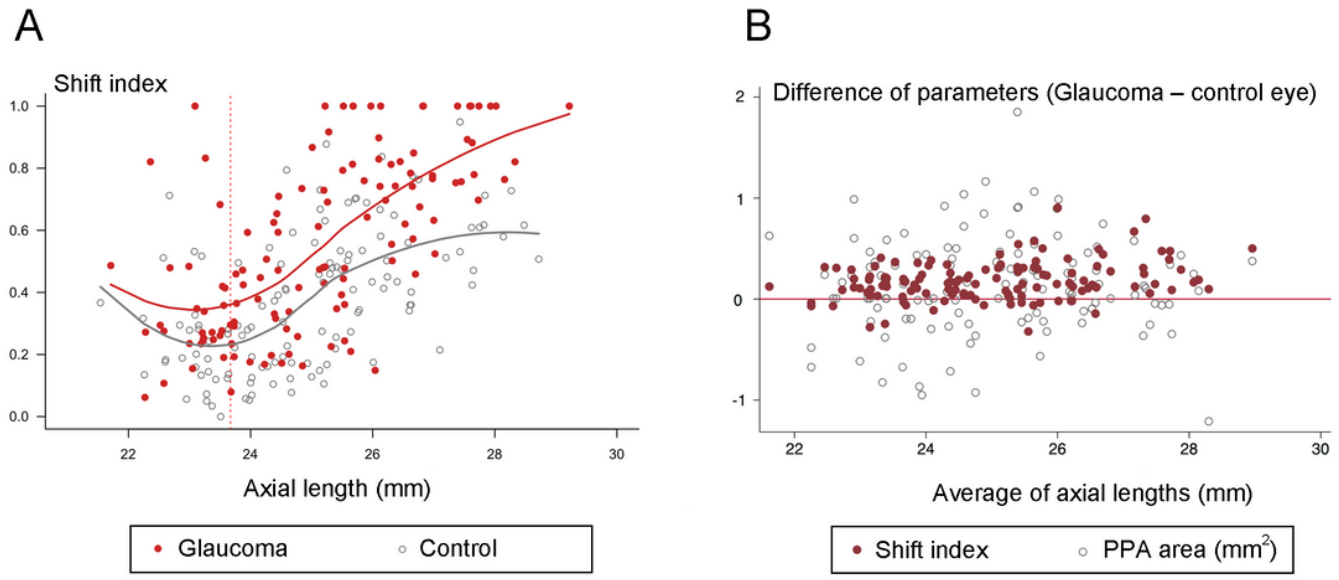

Figure 1

Shift index according to glaucoma diagnosis and axial length. (A) Scatter plot showing shift index according to diagnosis and axial length. Locally weighted scatterplot smoothing (LOESS) curves were fitted to describe the change of shift index depending on the axial length in each diagnosis. A generalized estimating equation (GEE) regression model revealed that the shift index was larger in the glaucoma eyes while it showed non-linear relationship with axial length (Table 3). The minimum value of shift index was anticipated at an axial length of 23.7 mm (red dashed vertical line). (B) Intra-individual difference of shift index and β-zone parapapillary atrophy (PPA) area. The difference was defined as the subtraction of values in the fellow control eyes from those in the glaucoma eyes. Along the reference line (red line), the upper side represents the larger value in glaucoma eyes, while the lower side the lesser value in glaucoma eyes. Compared with the differences of β-zone PPA areas, those of the shift index were located mostly on the upper side.

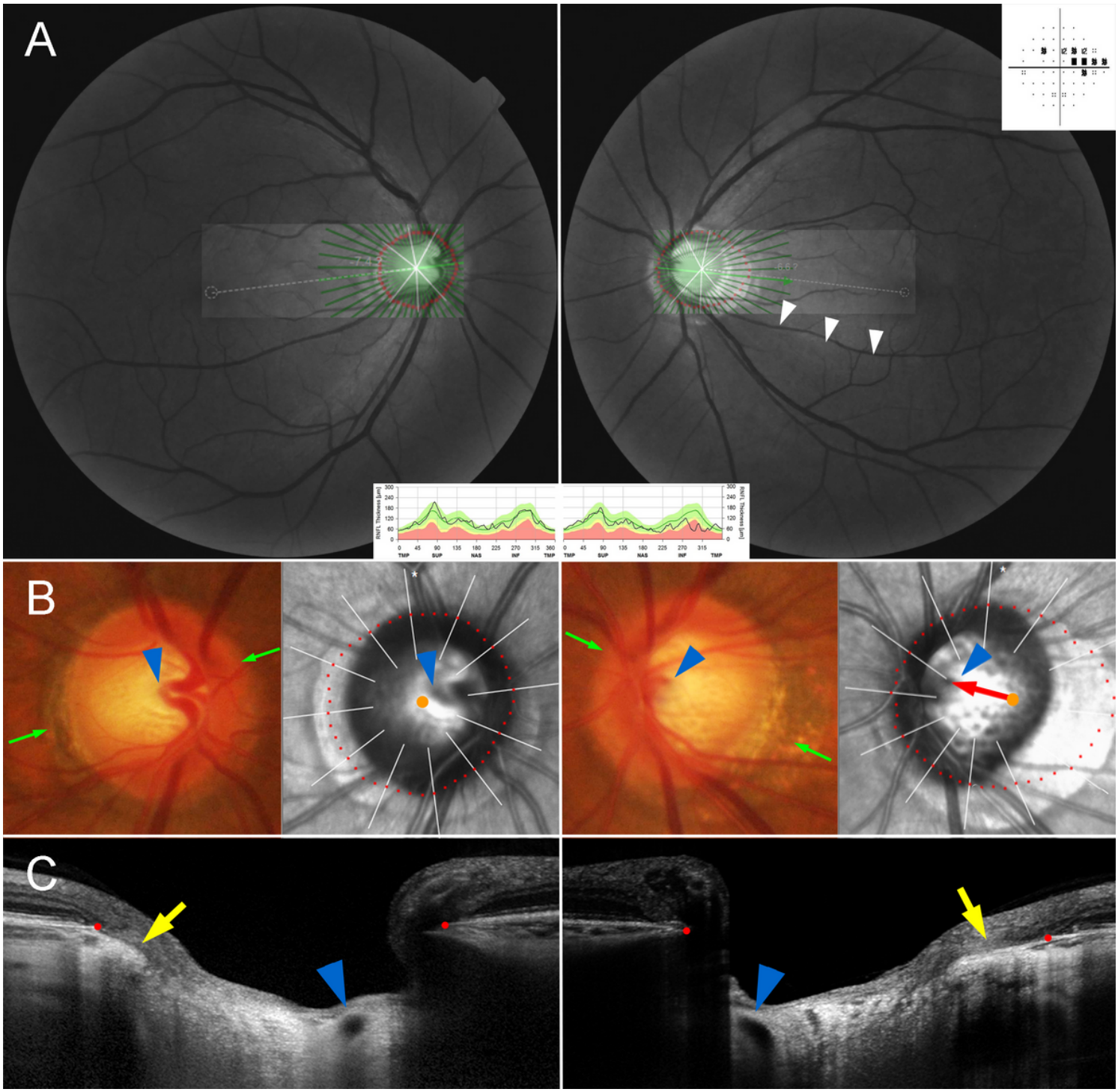

Figure 2

Inter-eye comparison of vascular trunk positions located on nasal side. (A) Red-free fundus photos and Humphrey visual field results. The infrared funduscopic spectral-domain (SD) OCT image is transposed to show the Bruch's membrane opening (BMO) margin (red dots). The red-free fundus photos show inferior retinal nerve fiber layer (RNFL) defect in the left eye only (white arrowheads). The Humphrey visual field results show superior scotomas corresponding to the RNFL defect. Circumpapillary RNFL thickness maps, as measured by SD-OCT, are given at the bottom for comparison. (B) Disc photographs and infrared fundus images. The red dots indicate the BMO margin. The orange dots indicate the centers

of the BMO. The arrowheads indicate the vascular trunk. The green arrows indicate the locations of the SD-OCT scans. Please note the larger shift in the glaucoma eye (red arrow). (C) B-scan SD-OCT images show emergence of vascular trunks (arrowheads). Please note the larger shift in the glaucoma eye as evidenced by the position of the vascular trunk (arrowheads) and the difference of the externally oblique borders (yellow arrows) on the temporal side.

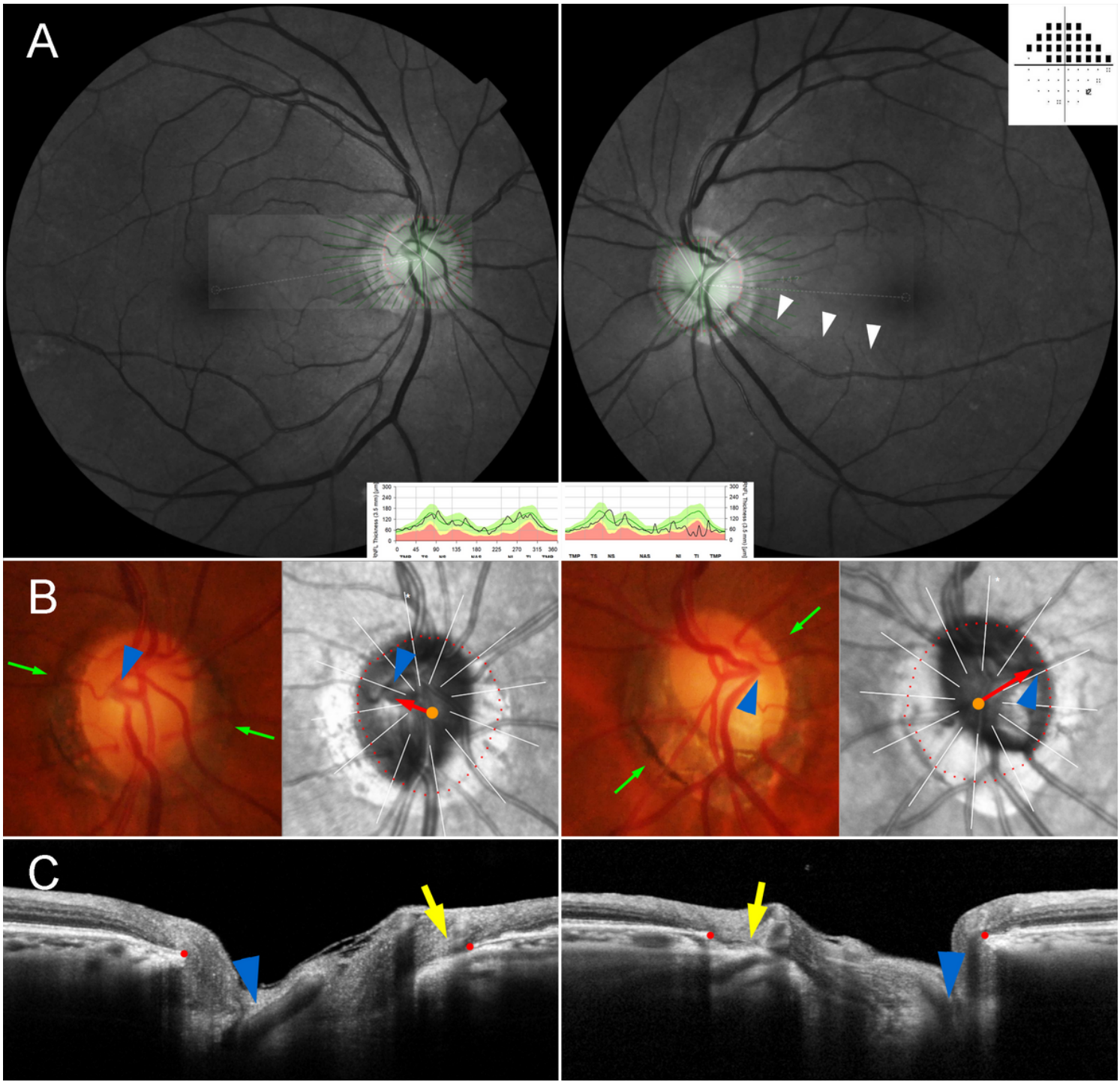

Figure 3

Inter-eye comparison of vascular trunk positions located on temporal side. (A) Red-free fundus photos and Humphrey visual field results. The infrared funduscopic spectral-domain (SD) OCT image is

transposed to show the Bruch's membrane opening (BMO) margin (red dots). The red-free fundus photos show inferior retinal nerve fiber layer (RNFL) defect in the left eye only (white arrowheads). The Humphrey visual field results show superior scotomas corresponding to the RNFL defect. Circumpapillary RNFL thickness maps, as measured by SD-OCT, are given at the bottom for comparison. (B) Disc photographs and infrared fundus images. The red dots indicate the BMO margin. The orange dots indicate the centers of the BMO. The arrowheads indicate the vascular trunk. The green arrows indicate the locations of the SD-OCT scans. Please note the larger shift in the glaucoma eye (red arrows). (C) B-scan SD-OCT images show emergence of vascular trunks (arrowheads). Please note the larger shift in the glaucoma eye as evidenced by the position of the vascular trunk (arrowheads) and the difference of the externally oblique borders (yellow arrows) on the nasal side.

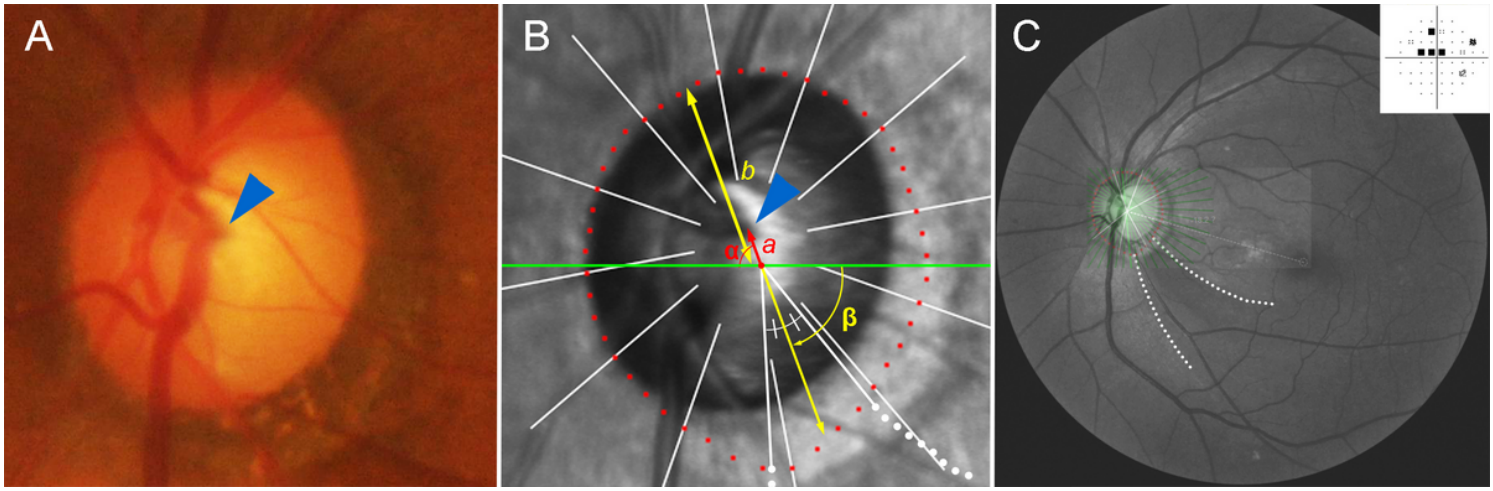

Figure 4

Measurement of central retinal vascular trunk deviation. (A) Disc photograph. The arrowhead indicates the emergence of the central retinal vascular trunk. (B) Infrared image obtained by spectral-domain optical coherence tomography (SD-OCT) with demarcated margin of Bruch's membrane opening (BMO). The red dots indicate the BMO margin, and the green line indicates the reference line. The angular deviation of the vascular trunk (α) is measured clock-wise, with the nasal horizontal midline as 0°. A positive value indicates the superior location, and a negative value indicates the inferior location relative to the reference line. The angular location of retinal nerve fiber layer (RNFL) defect (β) is measured clock-wise, with the temporal horizontal midline as 0°. A positive value indicates the superior location and a negative value indicates the inferior location relative to the reference line. From the BMO center, the distances are measured to the vascular trunk (a) and to the BMO margin in the same direction (b). The ratio of these distances was defined as the 'shift index' (a/b), which was used to measure the extent of shift. (C) Red-free fundus photo. A singular RNFL defect is observed in the inferior hemisphere (between the dotted lines). An infrared image is transposed to show the BMO margin. The Humphrey visual field result shows superior scotomas corresponding to the inferior RNFL defect.

Supplementary Files

This is a list of supplementary files associated with this preprint. Click to download.

- Table3.docx